

The emergence of polarization in coevolving networks

Jiazhen Liu,¹ Shengda Huang,^{1,*} Nathan Aden,¹ Neil Johnson,² and Chaoming Song^{1,†}

¹*Department of Physics, University of Miami, Coral Gables, Florida 33142, USA*

²*Physics Department, George Washington University, Washington D.C. 20052*

Abstract

Polarization is a ubiquitous phenomenon in social systems. Empirical studies show substantial evidence for opinion polarization across social media. Recent modeling works show qualitatively that polarization emerges in coevolving networks by integrating reinforcing mechanisms and network evolution. However, a quantitative and comprehensive theoretical framework capturing generic mechanisms governing polarization remains unaddressed. In this paper, we discover a universal scaling law for opinion distributions, characterized by a set of scaling exponents. These exponents classify social systems into polarization and depolarization phases. We find two generic mechanisms governing the polarization dynamics, and propose a coevolving framework that counts for opinion dynamics and network evolution simultaneously. We show analytically three different phases including polarization, partial polarization, and depolarization, and the corresponding phase diagram. In the polarized phase, our theory predicts that bi-polarized community structure emerges naturally from the coevolving dynamics. These theoretical predictions are in line with observations in empirical data for the Facebook and Blogosphere. Our theory not only accounts for the empirically observed scaling laws but also allows us to quantitatively predict scaling exponents.

* J.L. and S.H. contributed equally to the work.

† e-mail: c.song@miami.edu

Recently published discourse around opinion polarization, a process by which the opposition of opinions increases with time, has received much attention [1–4]. In particular, the political division between liberal and conservative parties reflects the heterogeneity in opinions regarding political orientations. These different attitudes are observed on social media [5–10], finding that the most frequently shared political opinions are aligned with a large proportion of the liberal or conservative population, i.e., the polarization of opinions.

Moreover, empirical studies show that the echo chamber effect underlies the opinion polarization in social networks [6, 7, 11, 12]. It suggests that like-minded users on social media tend to interact [5, 6, 13]. Indeed, the coexistence of polarization of opinions and network structures implies that the interplay between opinion and network dynamics plays an essential role in polarization. While growing coevolving models are proposed to understand mutual interactions between opinion and network structures, these studies did not focus specifically on opinion polarization [14–17]. Moreover, most of these models lack analytical solutions.

More recently, several coevolving models with a reinforcing mechanism show the emergence of polarization patterns numerically [18–21]. While theoretical analysis offers a qualitative understanding of the polarization patterns and the underlying network structures, exact solutions of reinforcement models are unknown. Furthermore, there are quantitative discrepancies between the empirical observations and reinforcement models. For instance, empirical data shows the existence of a depolarization phase where opinion distribution peaks around a neutral state with notable variance deviated from it [5], whereas previous reinforcement models reach a global consensus phase where everyone has the exact same opinion.

In this Letter, we report a universal scaling law characterized by a set of scaling exponents for empirical opinion distributions. These exponents classify social systems into polarization and depolarization phases. To explain this finding, we discover two ubiquitous mechanisms for the polarization dynamics: 1) *Opinion homogenization*. Individuals’ opinions are influenced by their neighbors in a social network and tend to converge to similar views [22–24], and 2) *Homophily clustering*. Social connections evolve with time, where individuals tend to connect to those with similar beliefs. Consequently, similar individuals group together to form clusters [6–8, 11]. These two mechanisms lead to the entanglement of network evolution with opinion dynamics. Therefore, we propose a generic coevolving framework that

captures the interplay between opinion dynamics and network evolution. We find the proposed framework’s exact solution and analytically predict the universal scaling laws observed in the empirical data. Furthermore, the model predicts three phases: (i) polarization, (ii) partial polarization, and (iii) depolarization. We calculate the phase diagrams analytically for the proposed model, validated by numerical simulation and empirical measurements. In particular, our new framework resolves the discrepancy between the empirical observations and the global consensus phase predicted by the existing models.

We use two datasets to uncover the patterns characterizing polarization. The first dataset consists of the 500 most shared online domains on Facebook between July 2014 to January 2015, collected by Bakshy et al. [5]. These domains are classified as either hard content (FB-HC) (such as national news, politics, or world affairs) or soft content (FB-SC) (such as sports, entertainment, or travel). For each domain, the proportion of different political viewpoints is measured [5], which allows us to compute the mean score of political leanings s for each domain, where s ranges from -1 (liberal) to 1 (conservative) continuously. The second dataset collected the Blogosphere (including eTalkingHead, BlogCatalog, CampaignLine, and Blogarama) ranging from 2004 to 2009 by Adamic and Glance [25]. This dataset consists of 1,490 blogs, and each blog has a list of references to other blogs. There are 19,090 references in the dataset, allowing us to reconstruct the social network. Each blog was classified by its political opinions into ‘liberal’ or ‘conservative.’ We assigned each blog an opinion score ranging from -1 to 1 to continuously quantify its political leaning (see SM Data Description and Processing for details).

We reconstruct the Blogosphere network Fig.1a, where nodes’ colors represents their political views. The redder (bluer) the node is, the more conservative (liberal) opinion it has, whereas the white color represents that its political stand is neutral. Figure 1a shows most nodes are deep red and blue colored, whereas only a few nodes are white. Moreover, the deep-colored nodes are clustered into two dense groups. These observation suggests that this network is polarized into two opposite communities, a phenomenon known as the echo chamber where people tends to favor/disfavor peers with similar/dissimilar opinions. [6, 7, 11, 12, 18].

To quantify the observed polarization, The scatter plots in Figure 2 depict the opinion distribution $P(s)$ for all three emprical datasets. We find that most users’ opinions in two political datasets (FB-HC and Blogosphere) are close to extreme values 1 and -1 , suggesting

these datasets are highly polarized. In contrast, most users' opinions stay neutral in the FB-SC dataset, with population size decreasing with the opinion extremeness. These findings indicate depolarization on the social platform focusing on sports, entertainment, and travel.

To investigate the scaling relation between the population size and opinion extremeness, we plot $P(s)$ as a function of $1 \pm s$ in the insets of Fig.2a-c, where $1 \pm s$ measures the opinion deviation from the most extreme ± 1 ones. We find

$$P(s) \sim (1 \mp s)^{\delta_{\pm}}, \quad (1)$$

satisfying power laws, where δ_{\pm} characterizes the power-law exponents when opinion s approaches ± 1 . While (1) applies equally to all empirical datasets, we find that exponents $\delta_{\pm} = -0.96 \pm 0.04$, $\delta_{\pm} = -0.72 \pm 0.04$ for FB-HC and $\delta_{\pm} = -0.94 \pm 0.16$, $\delta_{\pm} = -0.93 \pm 0.08$ for Blogosphere, whereas $\delta_{\pm} = 0.8 \pm 0.3$ for FB-SC. The negative exponent values indicate that the population increases with the extremeness of their opinions and diverges when the opinion score s reaches limiting cases ± 1 . In contrast, positive δ_{\pm} exponents indicate $P(s)$ is peaked around 0, i.e, the prominent population is neutral. Therefore, the exponents δ_{\pm} characterize polarization, i.e., $\delta_{\pm} < 0$ and > 0 for polarized and depolarized systems, respectively.

To explore the impact of the opinion's polarization on the network structure, we measured the average degree \bar{k} as a function of the opinion score s for the Blogosphere dataset. The scatter plot in Fig. 2d shows \bar{k} increases with the extremeness of opinion score s and reaches its maximum value when $s = \pm 1$, indicating that users who hold extreme political opinions are more likely to be the network's hubs. Indeed, Figure 1a shows that there are two loosely binding clusters, and most individuals in the same cluster are like-minded, suggesting polarization of the social network structures. To quantify the observed topology polarization, we measured the joint opinion distribution $Q(s, s')$ on each edge of the Blogosphere network, which computes the number of edges connected from an individual with opinion s to another with s' . Figure 2e plots the normalized joint opinion distribution $R(s, s') = Q(s, s')/P(s)P(s')$, measuring the deviations from the uncorrelated distribution [26]. We found a strong enhancement of the number of two connecting agents with similar opinions and suppression of the number of two connecting agents with dissimilar opinions. The two red spots are located in the regions corresponding to opposite political opinions, suggesting polarization in network topology. This observation indicates the existence of

homophily clustering in the real-world social network, in line with the echo chamber effect (Fig.1a).

To account for the empirical observations, we consider a coevolving network consisting of N interactive agents, each with an opinion s measures their view stands. Existing opinion models either use Boolean opinion values, i.e., $s = \pm 1$ [23], or a unbounded continuous variable [18–20]. However, empirical observations indicate that opinions are often quantified by continuous variables within a limited range. Therefore, we require the opinion s to vary continuously between -1 and 1 . Agents are connected through an underlining network described by its adjacency matrix A , where the matrix element $A_{ij} = 1$ or 0 represents the agent i being connected or disconnected to j . Both agents' opinions and the connections among them evolve in continuous time t . Moreover, we require the opinion dynamics and network evolution coupled together, satisfying two intrinsic mechanisms: 1) *Opinion homogenization*, that is, The change of an agent's opinion is largely influenced by the opinions of its neighbors and tends to change to similar views. 2) *Homophily clustering*, that describe the social connections being more likely established if agents hold similar views. The two mechanisms are coupled dynamically with the coevolution of both agents' opinions and social connections. Below we discuss this coevolution dynamics in detail.

Opinion homogenization. To model opinion homogenization, we assume the opinion dynamic follows stochastic process,

$$ds_i = \mu(s_i, \vec{s}, \mathbf{A})dt + \sigma(s_i)dW_t, \quad (2)$$

where $\vec{s} = (s_1, s_2, \dots, s_N)$ represents the set of opinions of all agents, and s_i is the opinion of agent i . \mathbf{A} is the adjacency matrix of the agents, and W_t is the standard Wiener process. μ is the drift term that controls the change of opinions on average, and σ is the diffusion term that controls the variance of opinion dynamics. Moreover, we assume that the opinion drift μ depends on the opinions of agent i and its neighbors, satisfying

$$\mu_i = \sum_{\langle i, j \rangle} F(s_i, s_j) = \sum_{j=1}^N A_{ij} F(s_i, s_j), \quad (3)$$

where $\langle i, j \rangle$ summing over interactions across all neighbors of i [22, 23, 27–30]. The pairwise force $F(s_i, s_j)$ quantifies the interaction between individuals i and j . The opinion homogenization requires $F(s, s) = 0$ and $\partial_s F(s, s') < 0$. On the other hand, the diffusion $D(s) \equiv \sigma(s)^2/2$ depends only on each agent's own opinion s . The boundness of opinion

requires the vanishing of the diffusion at the boundaries, i.e., $D(s = \pm 1) = 0$, implying a Taylor expansion, $D(s) = \frac{\sigma(s)^2}{2} = \frac{\sigma_0^2}{2}(1 - s^2) + O((1 - s^2)^2)$.

To solve Eq.(2), we start with the Fokker-Planck equation

$$\frac{\partial p(\vec{s}; t)}{\partial t} = - \sum_{i=1}^N \left[\frac{\partial}{\partial s_i} [\mu(\vec{s}, A) p(\vec{s}; t)] - \frac{\partial^2}{\partial s_i^2} [\alpha D(s_i) p(\vec{s}; t)] \right], \quad (4)$$

where $p(\vec{s}; t)$ is the opinion probability density for all agents at time t . For a sufficiently large N value, we introduce the single-agent opinion distribution $P(s; t) = \langle \sum_i \delta(s - s_i) / N \rangle_t$ and the joint opinion distribution $Q(s, s'; t) = \langle \sum_{i,j} A_{ij} \delta(s - s_i) \delta(s' - s_j) / N \rangle_t$, where $\langle \dots \rangle_t \equiv \int \dots p(\vec{s}, t) d\vec{s}$ denotes the ensemble average at time t . Substituting Eqs. (3–4), we obtain the time evolution for single-agent opinion (see SM Analytical Solutions for details),

$$\frac{\partial P(s; t)}{\partial (\alpha t)} = - \frac{\partial}{\partial s} \int_{-1}^1 F(s, s') Q(s, s'; t) ds' + \frac{\partial^2}{\partial s^2} [D(s) P(s; t)], \quad (5)$$

where the integral captures the neighboring interactions, since $Q(s, s'; t)$ depends on the underlying network \mathbf{A} implicitly.

Homophily clustering. To model homophily clustering, we assume that agents with similar opinions are more likely to connect to each other and less likely to break their relationships. To be specific, an agent i will connect to an unlinked agent j to construct a new edge with a probability rate $\gamma_+(s_i, s_j)$, where s_i and s_j are the opinions for agents i and j , respectively. At the same time, an agent i will disconnect with an linked agent j with probability rate $\gamma_-(s_i, s_j)$, leading to annihilating an existing edge. That is,

$$dP[A_{ij}(0 \rightarrow 1)] = \gamma_+(s_i, s_j) dt \quad (6a)$$

$$dP[A_{ij}(1 \rightarrow 0)] = \gamma_-(s_i, s_j) dt. \quad (6b)$$

If edge birth/death rates γ_{\pm} are constants, Equation (6) leads to a random graph, whereas γ_+ being proportional to the agent's degree reduces to the scale-free model [31]. To capture the homophily clustering, we assume that γ_{\pm} depend on the opinions of the agent i and its neighbors j . This dependency leads to the coupling of network evolution with opinion dynamics.

It is difficult to find the exact solution for Eq. (6) in its most general form. However, we notice that in most social media, the opinion changes are much slower than network evolution. To quantify their relative time scales, we rescale the opinion drift $F \rightarrow \alpha F$ and

diffusion $D \rightarrow \alpha D$ by a factor α that characterizes the opinion update rate relative to the network evolution. In terms of the power expansion of α , we find the time evolution of the joint opinion distribution $Q(s, s'; t)$ satisfies (see SM Analytical Solutions for details),

$$\frac{\partial Q(s, s'; t)}{\partial t} = \gamma_+(s, s')P(s; t)P(s'; t) - \gamma_-(s, s')Q(s, s'; t) + O(\alpha), \quad (7)$$

where $O(\alpha)$ term captures higher-order corrections. We will keep our discussion below at the limit $\alpha \rightarrow 0$, i.e., network evolves adiabatically, and $O(\alpha)$ will be omitted under this adiabatic approximation. Solving Eq. (5) together with Eq. (7) gives the full analytical results of the proposed framework.

Stationary solution. Below we will focus on the stationary solution of the proposed framework. Equation (7) leads to the stationary joint opinion distribution,

$$Q_{st}(s, s') = \frac{\gamma_+(s, s')}{\gamma_-(s, s')} P_{st}(s) P_{st}(s'), \quad (8)$$

where $P_{st}(s)$ is the stationary opinion distribution. Substituting Eq. (5) leads to

$$\int_{-1}^1 K(s, s') P_{st}(s') ds' = \ln(D(s) P_{st}(s)), \quad (9)$$

where the kernel $K(s, s') \equiv \int \frac{\gamma_+(s, s') F(s, s')}{\gamma_-(s, s') D(s)} ds$. When $s \rightarrow \pm 1$, we have $D(s) \rightarrow \frac{\sigma_0^2}{2}(1 - s^2) = \sigma_0^2(1 \mp s)$, and $K(s, s') \rightarrow \kappa_{\pm}(s') \ln(1 \mp s)$, where $\kappa_{\pm}(s') \equiv \frac{\gamma_+(\pm 1, s') F(\pm 1, s')}{\gamma_-(\pm 1, s') \sigma_0^2}$. Equation (9) becomes $\left(\int_{-1}^1 \kappa_{\pm}(s') P_{st}(s') ds' \right) \ln(1 \mp s) \sim \ln[(1 \mp s) P_{st}(s)]$. Therefore, our theory predicts the universal scaling law $P_{st}(s) \sim (1 \mp s)^{\delta_{\pm}}$, where the exponents

$$\delta_{\pm} = \int_{-1}^1 \kappa_{\pm}(s') P_{st}(s') ds' - 1, \quad (10)$$

in line with the scaling law discovered in empirical observations (1). This finding suggests that the universal scaling law is rather generic for coevolving networks and largely independent of microscopic details.

Opinion-topology correlation. Equation (8) indicates underlying correlations between the network structures and opinions. Indeed, empirical measure of the normalized joint opinion distribution $R(s, s') = Q(s, s')/P(s)P(s')$ (Fig.2e) of Blogosphere indicates that like-minded users tend to connect to each other, suggesting a bi-polarized community structure. Together with Eq.(8), our theory predicts $R(s, s') = \gamma_+(s, s')/\gamma_-(s, s')$. We will next investigate the dependence of agent's degree k on its opinion s . Since the joint opinion distribution $Q(s, s')$

counts for the number of edges connected by two agents' with opinions s and s' . Therefore the expected degree of an agent with opinion s , $\bar{k}(s)$ equals to the total number of edges with connected by it, that is, $\bar{k}(s) = \int_{-1}^1 Q(s'|s)ds' = \int_{-1}^1 Q(s, s')/P(s)ds'$. Together with Eq. (8), we find

$$\bar{k}(s) = \int_{-1}^1 ds' P_{st}(s') \gamma_+(s', s) / \gamma_-(s', s). \quad (11)$$

Equation (11) allows us to predict the correlation between network measure, \bar{k} , and opinion s .

Minimal Model. To compare our theory quantitatively with empirical data, below we will focus on a minimal realization of the proposed framework. To be specific, we use a linear opinion dynamics model [22, 23], $F(s, s') = \lambda(s' - s)$, where λ is a constant controlling the opinion change rate. We also assume the edge birth and death rates satisfies $\gamma_{\pm}(s, s') = r_{\pm}(1 + J_{\pm}ss')$, where $|J_{\pm}| \leq 1$ quantify the strength of homophily clustering, that is, similar individuals to establish their relationships. These assumptions serve as a minimal model of our theoretical framework. We find the explicit form of the kernel $K(s, s') = g \int \frac{1+J_{+}ss'}{1+J_{-}ss'} \frac{2(s'-s)}{1-s^2} ds$ for the minimal model (see SM Minimal Model), where the coupling constant $g \equiv \frac{\lambda}{\sigma_0^2} \frac{r_{+}}{r_{-}}$. Here $\frac{\lambda}{\sigma_0^2}$ represents the opinion homogenization rate and $\frac{r_{+}}{r_{-}}$ is the birth-death ratio for network connections. The coupling constant g integrates the interaction strengths of both opinion and network dynamics. Together with Eq.(9), we find the opinion distribution $P(s)$ analytically for the minimal model. We fit the empirical datasets with the proposed minimal model and find excellent agreements regarding the opinion distributions (green curves in Fig.2a-c). Equation (10) allows us to compute scaling exponents analytically. Figure 2a-c shows that our theoretical predictions (solid lines in insets) agree excellently with empirical measures.

To explore the opinion topology correlation, we plot the analytic prediction for $R(s, s') = \gamma_+(s, s')/\gamma_-(s, s')$ in Fig. 2f, showing that there are two highly clustered domains around the bottom-left and up-right corner. This finding indicates our model reproduces the real-world highly polarized topology structures (Fig 1b), in line with the community polarization observed in empirical data (Fig.2e). Moreover, the solid green curve in Fig.2d depicts the analytical prediction of Eq.(11), agreeing with the empirical measurement (scatter plot in Fig.2d). Moreover, this prediction suggests that our model generates two highly polarized clusters (Fig.1b), whose hubs show significant extremeness, in line with Fig.1a.

Phase diagram. As our theory successfully captures both U- and inverse U-shaped opinion distributions for polarized and depolarized phases, one may wonder how the modeling parameters control different phases. Below, we focus only on symmetric opinion distributions, i.e., $\langle s \rangle = 0$. We perform the numerical simulation of the minimal model with different g with fixed $J_+ = 0.7$ and $J_- = -0.8$. Figure 3a shows that a polarized U-shaped opinion distribution $P(s)$ emerges at a smaller g ($g = 0.9$). By gradually increasing the opinion change rate, we find that $P(s)$ transits from the U-shape to M-shape, indicating that the system is only partially polarized, in line with the previous empirical observations [18]. For sufficiently large g values ($g = 2.4$), $P(s)$ turns into a depolarized inverse U-shaped distribution.

As we discussed above, the exponent $\delta < 0$ for the polarized phase, whereas $\delta > 0$ for both partially and depolarized phases. Therefore, the transition between U- and M-shaped opinion distributions emerge when the exponent $\delta = 0$. Together with Eq. (10), we find the condition from polarized to partially polarized transition satisfies (see SM Phase Diagram)

$$g_*^{-1} + (J_+ - J_-)f(J_-) = 1, \quad (12)$$

where g_* represents the critical value of the coupling constant g for the phase transition from polarization to partial polarization, and $f(J_-) = (1 + J_-) \int_{-1}^1 ds' \frac{s'^2}{(1 - J_-^2 s'^2)} P_{st}(s')$.

For the transition between the partially polarized and depolarized phases, we notice that the first derivative at the $s = 0$ vanishes, i.e., $P'(0) = 0$ because of the symmetry. However, for the M-shaped $P(s)$ the second derivative $P''_{st}(0) > 0$, whereas $P''_{st}(0) < 0$ for inverse U-shaped $P(s)$. Therefore, the transition occurs when the second derivative vanishes, i.e., $P''_{st}(0) = 0$. Substituting $P'_{st}(0) = 0$ and $P''_{st}(0) = 0$ into Eq. (9), we obtain (see SM Phase Diagram)

$$g_{**}^{-1} + (J_+ - J_-)\langle s^2 \rangle = 1, \quad (13)$$

where g_{**} is the critical value of the coupling constant g for the phase transition from partial polarization to depolarization, and $\langle s^2 \rangle$ is the variance of the opinion distribution.

To quantify different phases, we define an order parameter $s_{max} = |\arg \max_s P(s)|$ as the most probable opinion. We find $s_{max} = 0$ for the depolarized phase (Fig. 3c), and $s_{max} = 1$ for the polarized phase (Fig. 3a). For the partially polarized phase, s_{max} are ranging between 0 and 1 (Fig. 3b), i.e., $0 < s_{max} < 1$. Figure 3d plots s_{max} as a function of the coupling constant g , indicating the existence of two phase transitions. The first phase transition occurs at the coupling constant $g_* \approx 1.3$, when s_{max} departs from 1, indicating

that the system transits from the polarization phase to partial polarization. The second phase transition occurs at $g_{**} \approx 1.78$, when s_{max} hits its minimal value 0, indicating the transition between the partial polarization and depolarization phases. Overall, decreasing the coupling constant g moves the system towards the polarization phase. Indeed, a smaller value of opinion homogenization rate drives agents' opinions far away from homogenization, heading to polarization. On the other hand, a larger birth-death ratio leads to a lower chance for agents with different opinions to be connected; hence, similar agents tends to cluster together with their opinions homogenized, eventually leading to the polarization phase.

To further explore the phase transitions, Figure 4 plots the phase diagram predicted by Eqs. (12-13), where the solid curves separate the domains corresponding to different phases. We also mark the empirical datasets in the diagram based on the modeling parameters fit from the data. The plot shows that Blogosphere and FB-HC are located at the polarization phase, whereas FB-SC is located at the depolarization phase. To further Eqs. (12-13), we approximate $P_{st}(s)$ at the critical points by a uniform distribution. This approximation leads to $\langle s^2 \rangle \approx 1/3$ and $f(J_-) \approx (1 + J_-)(J_- - \arctan(J_-))/J_-^3 = 1/3 + 1/3J_- + O(J_-^2)$. The dash lines in Fig.4 plots the predictions of this approximation, finding that it is consistent with the exact results (solid curves) when $J_+ - J_-$ is small.

In conclusion, we discover a universal scaling law for opinion distributions in real-world networks, characterized by a set of scaling exponents δ_{\pm} (Eq.10). This allows us to quantify different polarizing phases of the social system. We propose a generic framework for polarization dynamics of coevolving networks where opinion dynamics and network evolution are coupled based on two essential ingredients: 1) opinion homogenization and 2) homophily clustering. The proposed framework predicts three different polarizing phases and the corresponding phase diagram for modeling parameters. Our theory suggests that opinion homogenization rate and birth-death ratio are key parameters for the polarization dynamic, where a lower opinion homogenization rate and/or a larger edge birth-death ratio leads to polarization. Moreover, the exact solution of the theory reveals the observed scaling law for opinion distributions, suggesting the model captures the universal patterns of polarization successfully. Compared to existing models, we offer: (i) a generic and solvable modeling framework for polarization dynamics; (ii) the exact solution of the polarization phase diagram consisting of three different polarizing phases; and (iii) the analytical prediction of the universal

scaling laws for opinion distributions, with the prediction of corresponding scaling exponents. Many existing models can be treated as special cases of our modeling framework. For instance, the reinforcement model [18, 19] corresponds to $\mu(s_i, \vec{s}, \mathbf{A}) = s_i + \alpha \sum_j A_{ij} \tanh(s_j)$ and $\sigma(s) = 0$ in our framework. Unlike our minimal model, the vanishing $\sigma(s)$ term leads to the global consensus phase instead of the depolarized phase.

On the other hand, our analytic solution has been found under the adiabatic approximation, which assumes the opinion dynamic is much slower than the change of network structure. This assumption is reasonable for social media since individuals frequently follow or unfollow others but hardly change their viewpoints. It is still interesting to explore a more generic solution for the arbitrary opinion change rate. We will leave such possibilities for future investigations. Nevertheless, the current framework gives rise to precise prediction of polarization dynamics observed in the empirical data. As polarization takes place ubiquitously, our theory will serve as a starting point for future polarization studies in various systems. For example, recent studies show that opinions on different topics are commonly correlated [19, 32]. In this case, opinion can be modeled by a multidimensional variable. Such details can be readily incorporated into the proposed theoretical framework, which we plan to explore in a follow-up study.

Moreover, our theory offers a but also provides a generic framework for non-linear network dynamics, which can be used for many areas. For instance, by introducing $s = \cos(\theta)$, the framework leads to the models for synchronizations involving background changes [33–35].

Since polarization has drawn attentions from network science, social science and information science, our generic framework for polarization might have broad application across various fields. The exact solution of our theory accounts for the observed scaling law, promoting the understanding of polarization on complex systems.

ACKNOWLEDGMENTS

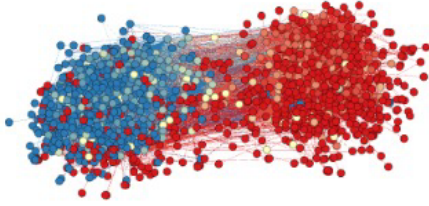
C.S. was supported partially by the National Science Foundation under Grant IBSS-1620294, the Institute of Education Sciences under Grant R324A180203, and the National

- [1] Aaron Bramson, Patrick Grim, Daniel J Singer, Steven Fisher, William Berger, Graham Sack, and Carissa Flocken. Disambiguation of social polarization concepts and measures. *The Journal of Mathematical Sociology*, 40(2):80–111, 2016.
- [2] Paul DiMaggio, John Evans, and Bethany Bryson. Have american’s social attitudes become more polarized? *American journal of Sociology*, 102(3):690–755, 1996.
- [3] Antonis Matakos, Evimaria Terzi, and Panayiotis Tsaparas. Measuring and moderating opinion polarization in social networks. *Data Mining and Knowledge Discovery*, 31(5):1480–1505, 2017.
- [4] Pedro D Manrique and Neil F Johnson. Individual heterogeneity generating explosive system network dynamics. *Physical Review E*, 97(3):032311, 2018.
- [5] Eytan Bakshy, Solomon Messing, and Lada A Adamic. Exposure to ideologically diverse news and opinion on facebook. *Science*, 348(6239):1130–1132, 2015.
- [6] Matteo Cinelli, Gianmarco De Francisci Morales, Alessandro Galeazzi, Walter Quattrociocchi, and Michele Starnini. The echo chamber effect on social media. *Proceedings of the National Academy of Sciences*, 118(9), 2021.
- [7] Michela Del Vicario, Alessandro Bessi, Fabiana Zollo, Fabio Petroni, Antonio Scala, Guido Caldarelli, H Eugene Stanley, and Walter Quattrociocchi. The spreading of misinformation online. *Proceedings of the National Academy of Sciences*, 113(3):554–559, 2016.
- [8] Kiran Garimella, Gianmarco De Francisci Morales, Aristides Gionis, and Michael Mathioudakis. Quantifying controversy on social media. *ACM Transactions on Social Computing*, 1(1):1–27, 2018.
- [9] Michela Del Vicario, Gianna Vivaldo, Alessandro Bessi, Fabiana Zollo, Antonio Scala, Guido Caldarelli, and Walter Quattrociocchi. Echo chambers: Emotional contagion and group polarization on facebook. *Scientific reports*, 6(1):1–12, 2016.
- [10] Javier Borge-Holthoefer, Walid Magdy, Kareem Darwish, and Ingmar Weber. Content and network dynamics behind egyptian political polarization on twitter. In *Proceedings of the 18th ACM Conference on Computer Supported Cooperative Work & Social Computing*, pages 700–711, 2015.

- [11] Kiran Garimella, Gianmarco De Francisci Morales, Aristides Gionis, and Michael Mathioudakis. Political discourse on social media: Echo chambers, gatekeepers, and the price of bipartisanship. In *Proceedings of the 2018 world wide web conference*, pages 913–922, 2018.
- [12] Wesley Cota, Silvio C Ferreira, Romualdo Pastor-Satorras, and Michele Starnini. Quantifying echo chamber effects in information spreading over political communication networks. *EPJ Data Science*, 8(1):1–13, 2019.
- [13] David Lazer, Alex Pentland, Lada Adamic, Sinan Aral, Albert-László Barabási, Devon Brewer, Nicholas Christakis, Noshir Contractor, James Fowler, Myron Gutmann, et al. Computational social science. *Science*, 323(5915):721–723, 2009.
- [14] Petter Holme and Mark EJ Newman. Nonequilibrium phase transition in the coevolution of networks and opinions. *Physical Review E*, 74(5):056108, 2006.
- [15] Gerardo Iniguez, János Kertész, Kimmo K Kaski, and Raphael Angl Barrio. Opinion and community formation in coevolving networks. *Physical Review E*, 80(6):066119, 2009.
- [16] Federico Vazquez, Juan Carlos González-Avella, Víctor M Eguíluz, and Maxi San Miguel. Time-scale competition leading to fragmentation and recombination transitions in the coevolution of network and states. *Physical Review E*, 76(4):046120, 2007.
- [17] Andreas Flache and Michael W Macy. Small worlds and cultural polarization. *The Journal of Mathematical Sociology*, 35(1-3):146–176, 2011.
- [18] Fabian Baumann, Philipp Lorenz-Spreen, Igor M Sokolov, and Michele Starnini. Modeling echo chambers and polarization dynamics in social networks. *Physical Review Letters*, 124(4):048301, 2020.
- [19] Fabian Baumann, Philipp Lorenz-Spreen, Igor M Sokolov, and Michele Starnini. Emergence of polarized ideological opinions in multidimensional topic spaces. *Physical Review X*, 11(1):011012, 2021.
- [20] Michele Starnini, Mattia Frasca, and Andrea Baronchelli. Emergence of metapopulations and echo chambers in mobile agents. *Scientific reports*, 6(1):1–8, 2016.
- [21] Kazutoshi Sasahara, Wen Chen, Hao Peng, Giovanni Luca Ciampaglia, Alessandro Flammini, and Filippo Menczer. Social influence and unfollowing accelerate the emergence of echo chambers. *Journal of Computational Social Science*, 4(1):381–402, 2021.
- [22] Peter Clifford and Aidan Sudbury. A model for spatial conflict. *Biometrika*, 60(3):581–588, 1973.

- [23] Richard A Holley and Thomas M Liggett. Ergodic theorems for weakly interacting infinite systems and the voter model. *The annals of probability*, pages 643–663, 1975.
- [24] Duncan Black. On the rationale of group decision-making. *Journal of political economy*, 56(1):23–34, 1948.
- [25] Lada A Adamic and Natalie Glance. The political blogosphere and the 2004 us election: divided they blog. In *Proceedings of the 3rd international workshop on Link discovery*, pages 36–43, 2005.
- [26] Sergei Maslov and Kim Sneppen. Specificity and stability in topology of protein networks. *Science*, 296(5569):910–913, 2002.
- [27] Guillaume Deffuant, David Neau, Frederic Amblard, and Gérard Weisbuch. Mixing beliefs among interacting agents. *Advances in Complex Systems*, 3(01n04):87–98, 2000.
- [28] Morris H DeGroot. Reaching a consensus. *Journal of the American Statistical Association*, 69(345):118–121, 1974.
- [29] Noah E Friedkin and Eugene C Johnsen. Social influence and opinions. *Journal of Mathematical Sociology*, 15(3-4):193–206, 1990.
- [30] Vishal Sood and Sidney Redner. Voter model on heterogeneous graphs. *Physical review letters*, 94(17):178701, 2005.
- [31] Albert-László Barabási and Réka Albert. Emergence of scaling in random networks. *science*, 286(5439):509–512, 1999.
- [32] Philipp Lorenz-Spreen, Bjarke Mørch Mønsted, Philipp Hövel, and Sune Lehmann. Accelerating dynamics of collective attention. *Nature communications*, 10(1):1–9, 2019.
- [33] Yoshiki Kuramoto. Self-entrainment of a population of coupled non-linear oscillators. In *International symposium on mathematical problems in theoretical physics*, pages 420–422. Springer, 1975.
- [34] Rodolphe Sepulchre, Derek A Paley, and Naomi Ehrich Leonard. Stabilization of planar collective motion: All-to-all communication. *IEEE Transactions on automatic control*, 52(5):811–824, 2007.
- [35] Kurt Wiesenfeld, Pere Colet, and Steven H Strogatz. Frequency locking in josephson arrays: Connection with the kuramoto model. *Physical Review E*, 57(2):1563, 1998.

FIGURES



(a) Blogosphere



(b) Model

FIG. 1. **Polarized networks.** (a) The Blogosphere network from 2004 to 2009. Colors represent political opinions, i.e., blue for liberals, red for conservatives, and white for neutral. (b) A social network generated by numerical simulations of our model for the polarization phase.

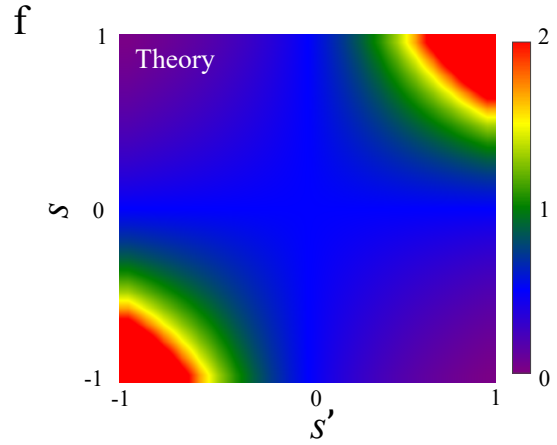
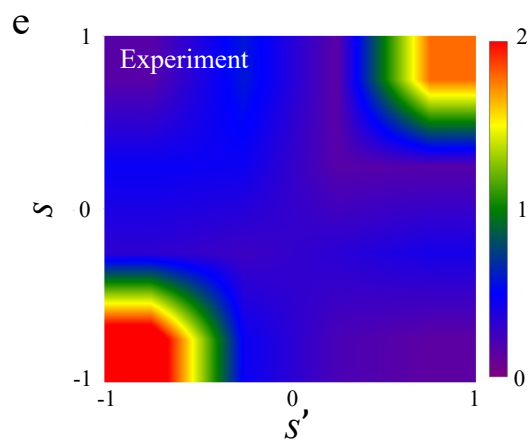
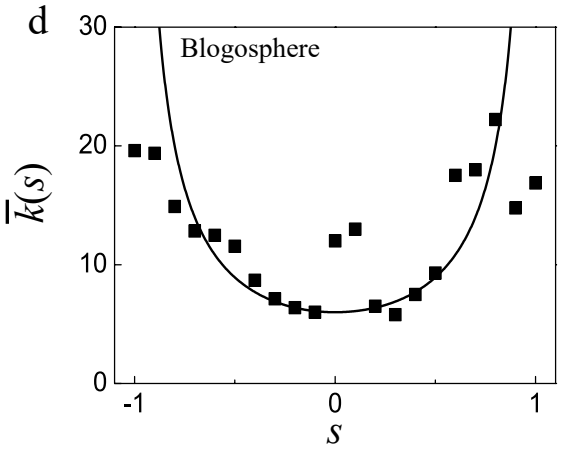
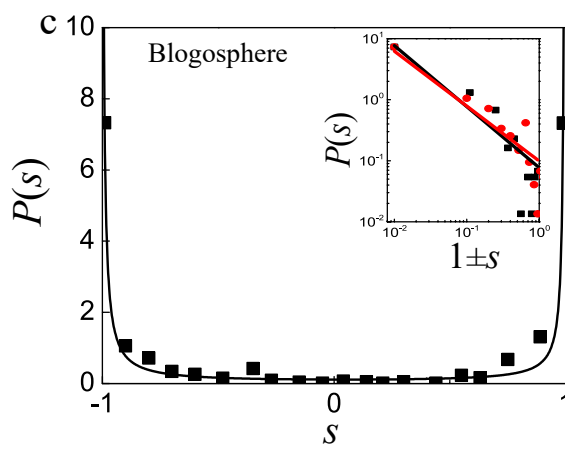
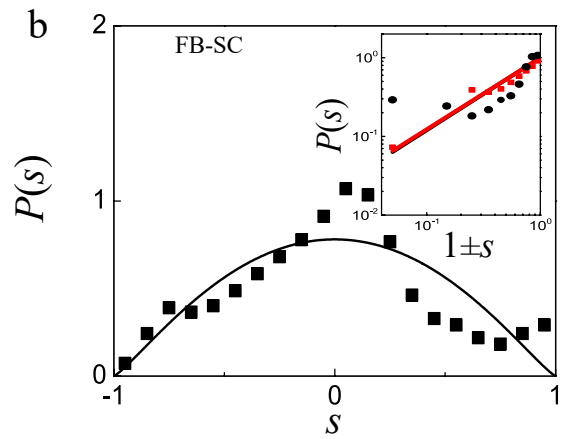
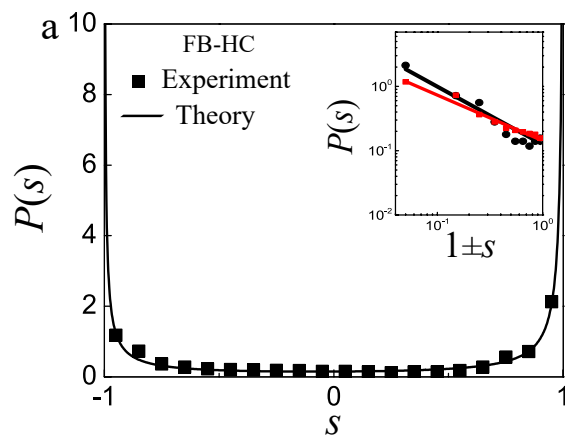


FIG. 2. **Theoretical results vs. empirical data.** (a)-(c) The empirical (dots) and theoretical results (green curves) of opinion distributions for FB-HC ($\langle s \rangle = 0.13, J_+ = 0.78, J_- = -0.8$ and $g = 0.05$), FB-SC ($\langle s \rangle = 0, J_+ = 0.3, J_- = -0.3$ and $g = 2.4$) and Blogosphere ($\langle s \rangle = 0.01, J_+ = 0.95, J_- = -0.95$ and $g = 0.01$). The horizontal axis of the insets is $1 \pm s$, measuring opinion deviation from the most extreme one. The scatter plots in the insets indicate that opinion distributions follow power laws, where FB-HC: $\delta_+ = -0.96 \pm 0.04, \delta_- = -0.72 \pm 0.04$; FB-SC: $\delta_{\pm} = 0.8 \pm 0.3$ and Blogosphere: $\delta_+ = -0.94 \pm 0.16, \delta_- = -0.93 \pm 0.08$. The solid lines represent our theoretical prediction (10) from our model, where FB-HC: $\delta_+ = -0.9, \delta_- = -0.71$; FB-SC: $\delta_{\pm} = 0.92$ and Blogosphere: $\delta_+ = -0.99, \delta_- = -0.92$. (d) The empirical results and theoretical predictions of the correlation between the network's degree and opinions for Blogosphere. (e)-(f) Heatmaps for the empirical and theoretical normalized joint-opinion distributions. These two plots indicate the similar opinions tend to link together, suggesting polarization of the network community, known as echo chamber.

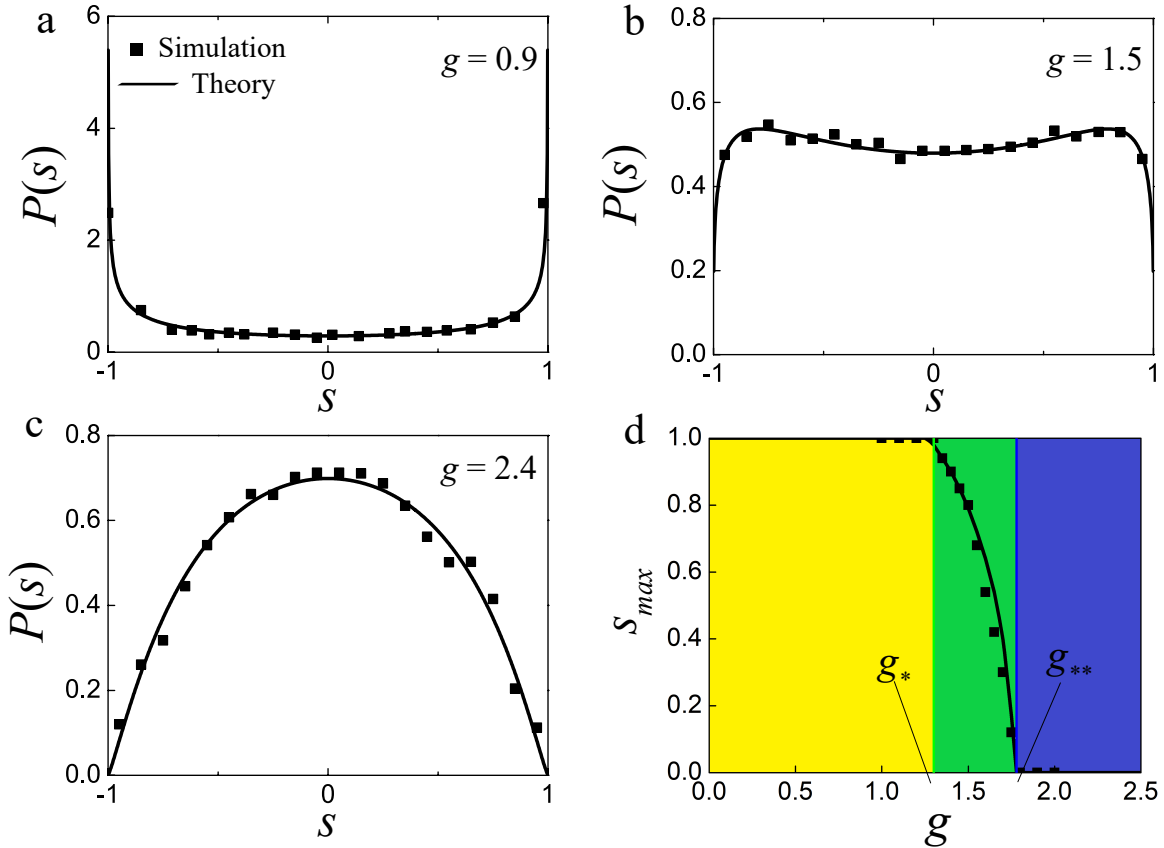


FIG. 3. **Phase transitions.** (a)-(c) The phase transition of opinion distributions with fixed $J_+ = 0.7$ and $J_- = -0.8$ ((a) Polarization: $g = 0.9$; (b) Partial polarization: $g = 1.5$; and (c) Depolarization: $g = 2.4$). (d) s_{max} against the coupling constant g . Here g_* and g_{**} are the critical values for phase transitions (g_* : polarization (yellow) to partial polarization (green); and g_{**} : partial polarization (green) to depolarization (blue)).

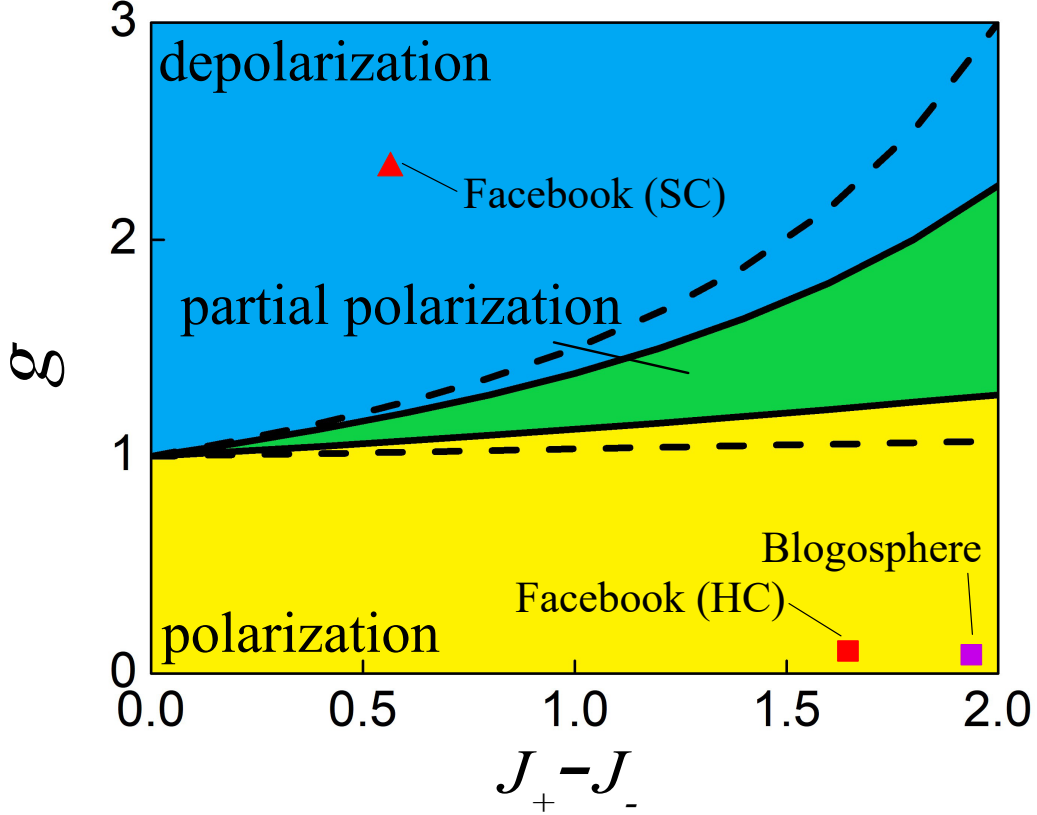


FIG. 4. **Phase diagram.** This figure shows the phase transition of opinion distributions with parameters g and J_{\pm} . The solid lines are the numerical results of Eqs.(12) and (13), representing the transition lines between depolarization (blue), partial polarization (green), and polarization (yellow). The dash lines are the analytical approximations of Eqs.(12) and (13). The red and purple squares (polarization) represent the real data for FB-HC and Blogosphere respectively, whereas the red triangle (depolarization) represents the data of FB-SC.